

# Role of Nitrides in Oxynitride Glasses and Glass-Ceramics: An NMR Investigation

Astrid Nordmann,<sup>\*,†</sup> Yi-Bing Cheng,<sup>†</sup> and Mark E. Smith<sup>‡</sup>

Department of Materials Engineering, Monash University, Clayton, Victoria 3168, Australia;  
CSIRO Division of Materials Science and Technology, Private Bag 33, Rosebank MDC,  
Clayton, Victoria 3169, Australia; and Physics Laboratory, University of Kent,  
Canterbury, Kent, CT2 7NR, U.K.

Received April 17, 1996. Revised Manuscript Received July 10, 1996<sup>§</sup>

Crystallization of nitrogen-containing glasses based on the  $\text{Li}_2\text{O}-\text{Al}_2\text{O}_3-\text{SiO}_2$  system produces materials comprised of  $\beta$ -quartz<sub>ss</sub> and  $\beta$ -spodumene<sub>ss</sub>, with minor amounts of X-phase ( $\text{Si}_3\text{Al}_6\text{O}_{12}\text{N}_2$ ) and silicon oxynitride ( $\text{Si}_2\text{N}_2\text{O}$ ). X-ray diffraction and <sup>29</sup>Si and <sup>27</sup>Al magic-angle spinning NMR spectroscopy have been used to study the effect of nitrogen on the thermal stability and atomic distribution of  $\beta$ -quartz<sub>ss</sub>, to monitor the evolution of secondary phases in the Li-Si-Al-O-N system, and to compare the differences between using  $\text{Si}_3\text{N}_4$  and AlN as the nitrogen source. Samples containing  $\leq 4$  wt % nitrogen and heat-treated at temperatures up to 1300 °C were analyzed by XRD to determine their crystallinity and phase content, whereas NMR was able to more clearly elucidate the atomic coordination and Si, Al distribution in the crystal structure.

## Introduction

In recent years many studies have focused on the preparation and characterization of oxynitride glasses and glass-ceramics. This interest has been sparked largely by the significant improvement in properties which may be achieved by partial substitution of oxygen by nitrogen. It is generally accepted that oxynitride glasses accommodate the trivalent nitrogen atoms via linkages to three Si atoms compared to the Si-O-Si nature of the pure oxide glass network. This alteration to the glass structure has strengthened the glass network and resulted in higher values of hardness,<sup>1,2</sup> Young's modulus,<sup>1,3</sup> and glass transition temperature<sup>4,5</sup> and in some instances has also facilitated the formation of oxynitride glass-ceramics.<sup>6-10</sup>

The lithium aluminosilicate (LAS) glass system is considered an ideal candidate from which to fabricate oxynitride glass-ceramics. With the aid of a nucleating agent, pure oxide LAS glasses are readily crystallized at temperatures between 700 and 1000 °C to produce  $\beta$ -quartz solid solution ( $\beta$ -quartz<sub>ss</sub>) and  $\beta$ -spodumene solid solution ( $\beta$ -spodumene<sub>ss</sub>) as the major crystalline

phases.<sup>11</sup> These materials have been widely used for domestic and industrial applications.  $\beta$ -Quartz solid solutions are derivatives of the high-quartz structure<sup>12</sup> and have the general composition  $\text{Li}_2\text{O}\cdot\text{Al}_2\text{O}_3\cdot n\text{SiO}_2$ , where  $n$  varies from 2 to 10.  $\beta$ -Spodumene solid solution is a stable crystal phase of composition  $\text{Li}_2\text{O}\cdot\text{Al}_2\text{O}_3\cdot(4-10)\text{SiO}_2$  and is a stuffed derivative of the tetragonal polymorph of silica known as keatite.<sup>13</sup> Thus, both can have the same composition (e.g.,  $\text{Li}_2\text{O}\cdot\text{Al}_2\text{O}_3\cdot 4\text{SiO}_2$ ) although  $\beta$ -quartz<sub>ss</sub> is often the preferred phase as it possesses a thermal expansion coefficient  $\alpha_{20-700^\circ\text{C}} = (0 \pm 0.15) \times 10^{-6} \text{ }^\circ\text{C}^{-1}$ , which is significantly lower than that of  $\beta$ -spodumene<sub>ss</sub>,  $\alpha_{20-700^\circ\text{C}} = (1-2) \times 10^{-6} \text{ }^\circ\text{C}^{-1}$  and hence offers better thermal shock resistance.<sup>14</sup> However, the transformation of  $\beta$ -quartz<sub>ss</sub> to  $\beta$ -spodumene<sub>ss</sub> has been reported to occur at temperatures below 900 °C,<sup>11,15</sup> and therefore the application temperatures of  $\beta$ -quartz<sub>ss</sub> are limited. Recent experimental evidence, however, has indicated that by incorporating small quantities of nitrogen into the LAS system the transformation can be delayed to temperatures as high as 1200 °C although details of the stabilization mechanism are still ambiguous.<sup>16</sup> The increase in the thermal stability of  $\beta$ -quartz<sub>ss</sub> suggests a potentially higher application temperature for this material. Consequently it is imperative that the role of nitrogen in oxynitride glasses and glass-ceramics is more clearly understood, not only to explain such stabilization effects in the LAS system but also to further develop the currently limited understanding of nitrogen-related effects in other oxynitride glass-ceramic systems.

Solid-state NMR is an atomic scale, element-specific probe that is able to identify local coordination environ-

<sup>†</sup> Monash University.

<sup>‡</sup> CSIRO Division of Materials Science and Technology and University of Kent.

<sup>§</sup> Abstract published in *Advance ACS Abstracts*, September 1, 1996.  
 (1) Loehman, R. E. *J. Non-Cryst. Solids* **1983**, *56*, 123.  
 (2) Hampshire, S.; Drew, R. A. L.; Jack, K. H. *J. Am. Ceram. Soc.* **1984**, *67*, C-46.  
 (3) Sakka, S.; Kamiya, K.; Yoko, T. *J. Non-Cryst. Solids* **1983**, *56*, 147.  
 (4) Unuma, H.; Kokubo, T.; Sakka, S. *J. Mater. Sci.* **1988**, *23*, 4399.  
 (5) Hampshire, S.; Drew, R. A. L.; Jack, K. H. *Phys. Chem. Glasses* **1985**, *26*, 182.  
 (6) Dinger, T. R.; Rai, R. S.; Thomas, G. *J. Am. Ceram. Soc.* **1988**, *71*, 236.  
 (7) Lonergan, J.; Morrissey, V.; Flynn, R.; Pomeroy, M.; Hampshire, S. *Key Eng. Mater.* **1992**, *72-74*, 145.  
 (8) Shaw, T. M.; Thomas, G.; Loehman, R. E. *J. Am. Ceram. Soc.* **1984**, *67*, 643.  
 (9) Messier, D. R.; Gleisner, R. P. *J. Am. Ceram. Soc.* **1988**, *71*, 422.  
 (10) Hu, G.; Yao, L.; Fang, Q.; Li, J. *J. Non-Cryst. Solids* **1986**, *80*, 209.

(11) Nordmann, A.; Cheng, Y.-B. *J. Mater. Sci.*, in press.

(12) Li, C.-T. *Z. Kristallogr.* **1968**, *127*, 327.

(13) Li, C.-T. *Z. Kristallogr.* **1968**, *126*, 46.

(14) Scheidler, H.; Rodek, E. *Am. Ceram. Soc. Bull.* **1989**, *68*, 1926.

(15) Lewis, M. H.; Metcalf-Johansen, J.; Bell, P. S. *J. Am. Ceram. Soc.* **1979**, *62*, 278.

(16) Unuma, H.; Miura, K.; Furusaki, T.; Kodaira, K. *J. Am. Ceram. Soc.* **1991**, *74*, 1291.

ments, usually via the isotropic chemical shift. Magic-angle spinning (MAS)<sup>17</sup> allows this isotropic information to be obtained more accurately by improving spectral resolution. In aluminosilicates and SiAlONs (silicon–aluminum–oxygen–nitrogen) that contain elements with very similar X-ray scattering factors, and where both atomic and structural order can occur, <sup>29</sup>Si and <sup>27</sup>Al MAS NMR have greatly contributed to new short-range structural insight.<sup>18</sup>  $\text{SiO}_4$  units with differing connectivity (termed  $Q^n$ , where  $n$  is the number of bridging bonds) and aluminum next-nearest neighbors ( $m$ ) can be readily distinguished in crystalline materials,<sup>19</sup> but for aluminosilicate glasses all these different resonances can blur together under chemical shift dispersion.<sup>19</sup> <sup>27</sup>Al provides an alternative perspective on the structure, but it suffers from broadening due to quadrupolar interactions which can be large enough that second-order effects become important. These are incompletely removed by MAS<sup>20</sup> and subtle structural changes are often not resolved although gross modifications (i.e.,  $\text{AlO}_4$  and  $\text{AlO}_6$  coordinations) are apparent. Structural and atomic disorder produces a distribution of quadrupolar interactions that result in asymmetric resonances.<sup>21</sup> Hence in crystalline but atomically disordered materials <sup>29</sup>Si is likely to be much more informative as the atomic disorder will give distinct resonances for the <sup>29</sup>Si but cause significant broadening of the <sup>27</sup>Al spectrum due to the range of quadrupole interactions generated.

In oxynitrides the nearest neighbour environment can also vary (e.g.,  $\text{SiO}_x\text{N}_{4-x}$ ) and the different <sup>29</sup>Si environments have been distinguished for yttrium<sup>22,23</sup> and lanthanum sialons.<sup>23,24</sup> The effect of nitrogen is smaller for  $\text{AlO}_x\text{N}_{4-x}$  units and the residual second-order quadrupolar broadening results in the separate resonances being poorly resolved.<sup>25-27</sup> In all these sialon-based systems there appears to be a tendency for silicon to become more highly coordinated by nitrogen compared to aluminum,<sup>25,26</sup> although how widely applicable and rigorous this rule is remains the subject of much debate.

In the present work solid-state <sup>29</sup>Si and <sup>27</sup>Al NMR techniques are applied to examine spodumene-based lithium sialon glasses and glass–ceramics to address the question of the effect of small amounts of nitrides on the structure of the crystalline phases and the changing nature of the Si, Al distribution and secondary phases formed with changing composition and heat treatment. NMR is able to probe both how the local structures of  $\beta$ -spodumene and  $\beta$ -quartz solid solutions are altered by this process and what minor secondary phases form. An understanding of the roles played by

**Table 1. Compositions of Glass Samples (wt %)**

sample	$\text{Li}_2\text{O}$	$\text{Al}_2\text{O}_3$	$\text{SiO}_2$	AlN	$\text{Si}_3\text{N}_4$	$N^a$
LAS	7.63	25.99	66.38			
2NAN	7.18	24.48	62.79	5.85		2
3NAN	6.95	23.71	60.99	8.78		3
4NAN	6.73	22.95	59.18	11.71		4
2NSN	7.25	24.69	63.31		5.00	2
4NSN	6.87	23.39	60.24		10.00	4

<sup>a</sup> Indicates the effective nitrogen content that results from the corresponding addition of AlN or  $\text{Si}_3\text{N}_4$ .

AlN and  $\text{Si}_3\text{N}_4$  in this system is clearly vital to a coherent approach to improved material performance.

## Experimental Section

**Materials Processing.** As outlined in a previous study<sup>11</sup> oxide glasses were prepared by melting approximately 100 g of spodumene concentrate (95 wt %  $\text{LiAlSi}_2\text{O}_6$ , 5 wt %  $\text{SiO}_2$ , Gwalia Australia Ltd.) in a Pt crucible at 1600 °C for 3 h, followed by water quenching. The glass was subsequently crushed and remelted under the same conditions twice more to ensure homogeneity.

After grinding the oxide glass to a fine powder it was combined with appropriate quantities of  $\text{Si}_3\text{N}_4$  (Starck Berlin Grade LC10) or AlN (Stark Berlin Grade C) to form the compositions given in Table 1. As indicated, the compositions were designed to produce oxynitride glasses containing up to 4 wt % nitrogen using either  $\text{Si}_3\text{N}_4$  or AlN as the nitrogen source. Although it is common practice in the study of oxynitride materials to fix the cation content so that structural changes with varying nitrogen content may be monitored, this has not been done in the present study since it forms part of an overall investigation that examines the processing of glasses and glass–ceramics from spodumene minerals. To compensate for the increased cation content that results from the addition of  $\text{Si}_3\text{N}_4$  or AlN to the mineral, it would have been necessary to simultaneously add additional powders to the initial batch to rectify such an imbalance. Consequently, Table 1 lists the compositions of glasses containing (100 –  $x$ ) wt % spodumene concentrate and  $x$  wt %  $\text{Si}_3\text{N}_4$  or AlN to yield nitrogen concentrations of 2, 3, and 4 wt %. The average weight losses that occurred during glass fabrication for both the  $\text{Si}_3\text{N}_4$  and AlN series of samples were comparable and were also quite small (<1%), which suggests that the compositions were close to those designed.

The nitrogen-containing powders were combined with the LAS glass powder and mixed in an agate mortar and pestle with a small amount of 2-propanol added to aid mixing. After evaporation of the alcohol the mixture was uniaxially compressed to form pellets approximately 14 mm in diameter and 10 mm high. The green compacts were contained in a BN-lined graphite crucible and melted in an induction heated graphite furnace at 1600 °C under a nitrogen atmosphere. The samples were held at this temperature for 30 min and then were furnace cooled at a rate of approximately 150 °C/min to form oxynitride glasses. Oxynitride glass–ceramics were prepared by heat-treating the glass samples in a Lindberg laboratory tube furnace at the specified temperatures for 4 h. A heating and cooling rate of 1 °C/min was employed and a constant flow of high-purity nitrogen was maintained through the furnace for the duration of the heat treatment. The pure oxide glass–ceramics used as reference materials (i.e.,  $\beta$ -quartz<sub>ss</sub> and  $\beta$ -spodumene<sub>ss</sub>) were prepared according to the description given in ref 28.

**Materials Characterization.** XRD experiments were performed at room temperature (22 °C) using a Rigaku Geigerflex diffractometer operating at 40 kV and 22.5 mA and using Ni-filtered  $\text{Cu K}\alpha$  radiation of wavelength 0.1541 nm. The samples were crushed to a fine powder and scanned at 0.2°/min using a step size of 0.01°.

- (17) Andrew, E. R. *Int. Rev. Phys. Chem.* **1981**, 1, 195.
- (18) Eckert, H. *Prog. NMR Spectrosc.* **1992**, 24, 159.
- (19) Engelhardt, G.; Michel, D. *High Resolution NMR of Silicates and Zeolites*; Wiley: Chichester, 1987.
- (20) Smith, M. E. *Appl. Magn. Reson.* **1993**, 4, 1.
- (21) Jaeger, C.; Kunath, G.; Losso, P.; Scheler, G. *Solid State NMR* **1993**, 2, 73.
- (22) Dupree, R.; Lewis, M. H.; Smith, M. E. *J. Am. Chem. Soc.* **1988**, 110, 1083.
- (23) Harris, R. K.; Leach, M. J.; Thompson, D. P. *Chem. Mater.* **1989**, 1, 336.
- (24) Dupree, R.; Lewis, M. H.; Smith, M. E. *J. Am. Chem. Soc.* **1989**, 111, 5125.
- (25) Dupree, R.; Lewis, M. H.; Smith, M. E. *J. Appl. Crystallogr.* **1988**, 21, 1083.
- (26) Smith, M. E. *J. Phys. Chem.* **1992**, 96, 1444.
- (27) Fitzgerald, J. J.; Kohl, S. D.; Piedra, G.; Dec, S. F.; Maciel, G. E. *Chem. Mater.* **1994**, 6, 1915.

- (28) Nordmann, A.; Cheng, Y.-B.; Bastow, T. J.; Hill, A. J. *J. Phys.: Condens. Matter* **1995**, 7, 3115.

**Table 2. Phase Content of Oxide and Oxynitride Glasses Heat-Treated for 4 h at the Given Temperatures<sup>a</sup>**

sample	1000 °C					1200 °C					1300 °C				
	Q	S	X	O	g	Q	S	X	O	g	Q	S	X	O	g
LAS oxide		vs					vs					vs			
2NAN	vs					w	vs	vw				vs	w	vw	
3NAN	vs	w		vw		mw	s	vw	w						
4NAN	vs	w	vw	vw		mw	m	vw	w		m	m	w	w	
2NSN	ms	m				vw	vs		vw						
4NSN	mw	s			/	w	vs								

<sup>a</sup> Q =  $\beta$ -quartz<sub>ss</sub>, S =  $\beta$ -spodumene<sub>ss</sub>, X = X-phase [Si<sub>3</sub>Al<sub>6</sub>O<sub>12</sub>N<sub>2</sub>], O = Si<sub>2</sub>N<sub>2</sub>O, g = glass. X-ray intensities: vs = very strong; s = strong; ms = medium strong; m = medium; mw = medium weak; w = weak; vw = very weak.

<sup>29</sup>Si MAS NMR was performed on a Bruker CXP 300 spectrometer controlled by a Tecmag miniMacSpect unit and equipped with a 7.05 T magnet. The system was operated at 59.61 MHz with the samples spun in a 7 mm double-bearing (DB) MAS NMR probe at 4–5 kHz. Short 1.5  $\mu$ s pulses (corresponding to  $\sim$ 30° tip angle) with a recycle delay of 60 s were used. These conditions were chosen as a compromise to obtain an adequate signal-to-noise ratio although some minor saturation may occur. The spectra were referenced against an external standard of tetramethylsilane at 0 ppm. The <sup>27</sup>Al MAS NMR spectra were collected on a Bruker MSL 400 spectrometer operating at 104.2 MHz in a magnetic field of 9.4 T. A 4 mm DB-MAS probe was used with a spinning speed in excess of 10 kHz. A short 0.7  $\mu$ s ( $\sim$ 15°) pulse and 1 s recycle delay ensured completely relaxed, quantitative spectra. The spectra were referenced against an external standard of Y<sub>3</sub>Al<sub>5</sub>O<sub>12</sub>, with the AlO<sub>6</sub> resonance taken as 0.7 ppm.

## Results

**XRD.** Table 2 summarizes the phases formed when the oxynitride glasses were heat-treated for 4 h at 1000, 1200, and 1300 °C, respectively. The results for the nitrogen-free oxide glass are also included in this table.

Differences in phase evolution arose as the heat-treatment temperature, sample composition, and nitrogen source were varied. For composition 2NAN heat-treated at 1000 °C,  $\beta$ -quartz<sub>ss</sub> was the only crystalline phase observed. As the temperature increased to 1200 °C,  $\beta$ -quartz<sub>ss</sub> transformed to  $\beta$ -spodumene<sub>ss</sub> so that only weak  $\beta$ -quartz<sub>ss</sub> reflections were detected, and X-phase evolved as a minor constituent as well. By 1300 °C,  $\beta$ -quartz<sub>ss</sub> had fully transformed to  $\beta$ -spodumene<sub>ss</sub>, although weak reflections corresponding to X-phase and Si<sub>2</sub>N<sub>2</sub>O were still observed. At no stage did the XRD spectra indicate the presence of glass in the AlN-containing 2NAN series of samples, as judged by the lack of a broad background peak at low 2 $\theta$  angles.

Sample 2NSN, which also contained 2 wt % nitrogen but relied on Si<sub>3</sub>N<sub>4</sub> rather than AlN as the nitrogen source, displayed different crystallization behavior. Heat-treatment of 2NSN at 1000 °C led to the formation of both  $\beta$ -quartz<sub>ss</sub> and  $\beta$ -spodumene<sub>ss</sub>, with no minor phases detected. This contrasts sharply with 2NAN in which only  $\beta$ -quartz<sub>ss</sub> was formed at this temperature. Increasing the 2NSN heat-treatment temperature to 1200 °C resulted in almost total conversion of  $\beta$ -quartz<sub>ss</sub> to  $\beta$ -spodumene<sub>ss</sub>, and Si<sub>2</sub>N<sub>2</sub>O was detected as a minor phase. As for 2NAN, no glass was detected in the 2NSN samples according to XRD, regardless of the heat-treatment temperature used.

For samples containing a higher nitrogen content (i.e., 3–4 wt %) different crystallization behavior was observed. For example, in sample 4NAN, all four crystalline phases ( $\beta$ -quartz<sub>ss</sub>,  $\beta$ -spodumene<sub>ss</sub>, X-phase, and Si<sub>2</sub>N<sub>2</sub>O) coexisted at all heat-treatment temperatures, albeit in different proportions. X-phase and Si<sub>2</sub>N<sub>2</sub>O

were only minor constituents at any given temperature, but differences arose in the relative amounts of  $\beta$ -quartz<sub>ss</sub> and  $\beta$ -spodumene<sub>ss</sub>. At 1000 °C,  $\beta$ -quartz<sub>ss</sub> was the dominant phase with only a weak contribution from  $\beta$ -spodumene<sub>ss</sub>, and with increasing temperature to 1200 and 1300 °C  $\beta$ -spodumene<sub>ss</sub> formed at the expense of  $\beta$ -quartz<sub>ss</sub>. At no stage was any glass detected in the 4NAN samples.

Sample 4NSN, which contained 4 wt % nitrogen derived from Si<sub>3</sub>N<sub>4</sub>, was the only sample studied which contained both  $\beta$ -quartz<sub>ss</sub> and  $\beta$ -spodumene<sub>ss</sub> as well as residual glass at 1000 °C. When the heat-treatment temperature was increased to 1200 °C, almost total conversion to  $\beta$ -spodumene<sub>ss</sub> had taken place. At no time did the 4NSN samples exhibit X-phase or Si<sub>2</sub>N<sub>2</sub>O as minor constituents. From these results it becomes clear that the stability of crystalline phases depends not only on the amount of nitrogen present but also on the type of nitride used to introduce nitrogen into the glasses.

**NMR.** <sup>29</sup>Si and <sup>27</sup>Al MAS NMR results provide atomic scale information that can be combined with the complementary information from XRD to build a comprehensive picture of the phases present and their structures. Figure 1 shows <sup>29</sup>Si MAS NMR spectra from the pure oxide  $\beta$ -quartz<sub>ss</sub> (a) along with the spectra recorded from samples that were heat treated for 4 hours at 1000 °C and contained 2, 3 and 4 wt % nitrogen due to the addition of AlN (b-d). The well resolved <sup>29</sup>Si MAS NMR spectra immediately indicate the crystalline nature of these phases. Although the presence of  $\beta$ -spodumene<sub>ss</sub> cannot be discounted and would to a large extent overlap the spectrum from the  $\beta$ -quartz<sub>ss</sub> there is little evidence of any significant spectral contribution from  $\beta$ -spodumene<sub>ss</sub>. The  $\beta$ -quartz<sub>ss</sub> shows a distinctive spectrum with five resonances at  $\sim$ 91.1,  $\sim$ 97.5,  $\sim$ 102.7,  $\sim$ 108.4, and  $\sim$ 115.5 ppm (the first only appears as a shoulder and to ascertain its position accurately requires spectral simulation by Gaussians as described previously<sup>19,28</sup>). It is interesting to contrast this spectrum with that published on essentially an identical sample but at a higher applied magnetic field where the resolution was clearer.<sup>28</sup> For example the lower intensity outer two peaks are readily resolved at the higher field. This is an indication of the advantage of higher applied magnetic fields (9.4 T compared to 7.05 T) at enhancing resolution, as the separation of the peaks (in ppm) remains constant, while the line width (in ppm) decreases with increasing field. As nitrogen is added (in the form of AlN), the spectra show distinct changes in the relative intensities of the peaks, while the actual peak positions remain constant. It is also significant that there is some ill-defined intensity below  $\sim$ 90 ppm for the nitrogen-containing systems that is

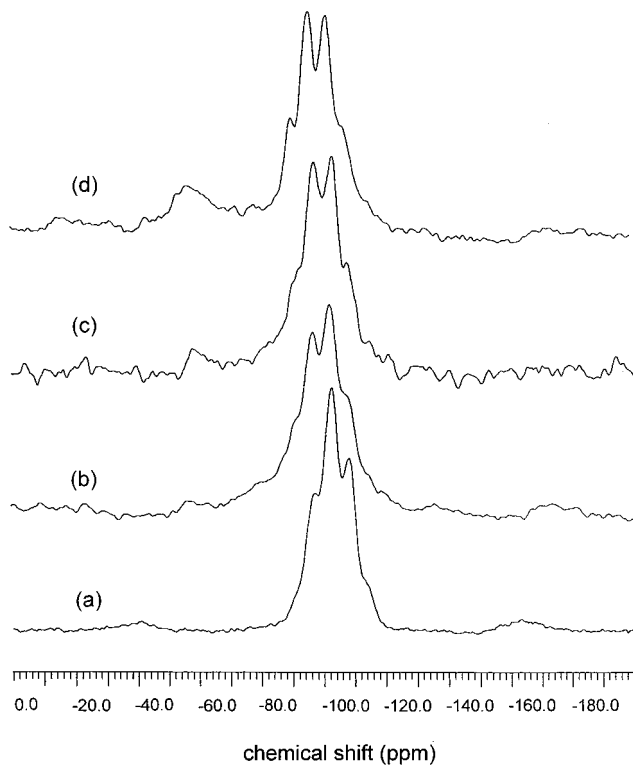


**Figure 1.**  $^{29}\text{Si}$  MAS NMR spectra of (a)  $\beta$ -quartz<sub>ss</sub> and (b) 2NAN, (c) 3NAN, and (d) 4NAN samples heat-treated at 1000 °C.

absent from the pure oxide  $\beta$ -quartz<sub>ss</sub>. In addition, for the nitrogen-containing samples there is a separate minor peak at -60 ppm that increases in intensity with increasing nitrogen content, and which is not a spinning sideband since the first sideband is well removed at more positive shift than -40 ppm.

Heat-treating 2NAN causes significant changes in the  $^{29}\text{Si}$  MAS NMR spectra (Figure 2) compared to that obtained at 1000 °C, with the main peak evident at  $\sim$ -100 ppm and with other shoulders appearing at  $\sim$ -95 and -107.6 ppm. For 2NAN both at 1200 °C (Figure 2a) and 1300 °C (Figure 2b), the spectra remain unchanged with the peak around -100 ppm. The overall shape is now characteristic of  $\beta$ -spodumene<sub>ss</sub> but with the component resonances having slightly different relative intensities from the pure oxide  $\beta$ -spodumene<sub>ss</sub> with the less shielded peaks increasing. The  $^{29}\text{Si}$  spectra recorded from 4NAN at 1200 and 1300 °C remain characteristic of  $\beta$ -quartz<sub>ss</sub>, although the presence of some  $\beta$ -spodumene<sub>ss</sub> cannot be discounted. 2NAN heat-treated at 1200 and 1300 °C shows a weak resonance at  $\sim$ -60 ppm at both temperatures. This peak is much more prominent in the higher nitrogen-containing 4NAN at the same temperatures. The evolution of the intensity below -80 ppm is also interesting. At 1000 °C the peak at -60 ppm is much less well defined, and there was some weak intensity extending from the main resonance to -60 ppm. However, on heat treatment the intermediate intensity is largely eliminated and the peak at -60 ppm increases substantially in relative intensity, appearing to be still increasing at 1300 °C.

Using  $\text{Si}_3\text{N}_4$  as the source of nitrogen in the samples produces markedly different  $^{29}\text{Si}$  NMR spectra for the same heat treatment compared to AlN. 2NSN at 1000 °C for 4 h (Figure 3b) shows resolution and peak

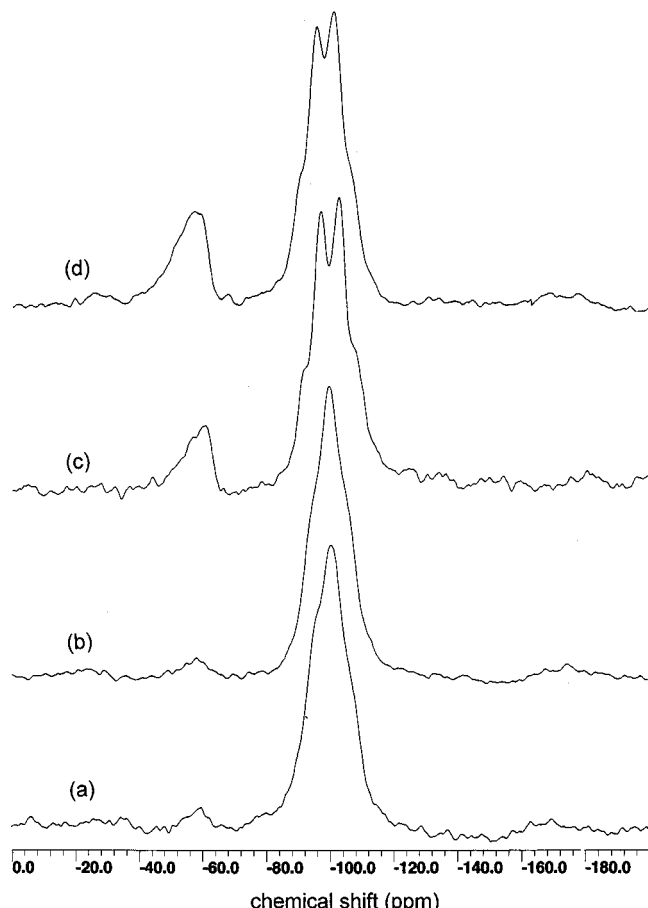


**Figure 2.**  $^{29}\text{Si}$  MAS NMR spectra of 2NAN heat-treated at (a) 1200 °C and (b) 1300 °C and 4NAN heat-treated at (c) 1200 °C and (d) 1300 °C.

positions characteristic of  $\beta$ -quartz<sub>ss</sub>. There is also a very broad tail extending from -70 to -90 ppm and no intensity around -60 ppm. Heating to 1200 °C converts the spectrum to that characteristic of  $\beta$ -spodumene<sub>ss</sub> with a very small peak at -60 ppm (Figure 3c). The 4NSN sample heated to 1000 °C makes an interesting comparison and shows a much broader ill-defined peak (Figure 3d), characteristic of an aluminosilicate glass that results in a reduced signal-to-noise ratio. Heating to 1200 °C produces a  $^{29}\text{Si}$  NMR spectrum of  $\beta$ -spodumene<sub>ss</sub> (Figure 3e) as the major resonance but with an additional peak at  $\sim$ -60 ppm.

$^{27}\text{Al}$  MAS NMR spectra from samples heated to 1000 °C under nitrogen are shown and compared to the pure oxide  $\beta$ -quartz<sub>ss</sub> (Figure 4). The  $\beta$ -quartz<sub>ss</sub>  $^{27}\text{Al}$  MAS NMR spectrum is very similar to that previously observed in the oxide systems<sup>28</sup> except that here a small amount of  $\text{AlO}_6$  is present. It should be emphasized that this corresponds to a very minor amount as it sits on the tail of the dominant  $\text{AlO}_4$  resonance that peaks at 45.5 ppm. Introduction of nitrogen causes small differences although the spectra continue to be dominated by  $\text{AlO}_4$  which progressively shifts to 49 and 51.5 ppm in 2NAN and 4NAN respectively (Figure 4b,c). 4NAN also shows a small amount of  $\text{AlO}_6$  at around 2 ppm with some additional intensity that extends to positive shift from the main  $\text{AlO}_4$  resonance up to around 80 ppm. Again the samples with added  $\text{Si}_3\text{N}_4$  are a little different with the main peaks at  $\sim$ 50 ppm and no evidence of  $\text{AlO}_6$  sites at 1000 °C. 4NSN has

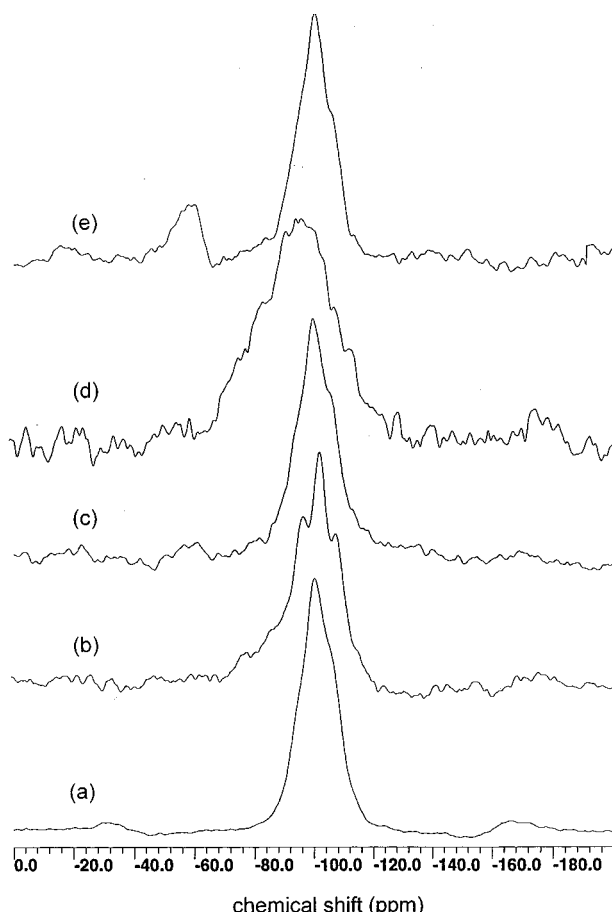


**Figure 3.**  $^{29}\text{Si}$  MAS NMR spectra of (a)  $\beta$ -spodumene<sub>ss</sub>; 2NSN heat-treated at (b) 1000 °C and (c) 1200 °C; 4NSN heat-treated at (d) 1000 °C and (e) 1200 °C.

some weak intensity at positive shift but not to the extent of 4NAN.

### Discussion

XRD demonstrates that sample 4NSN heat-treated at 1000 °C shows significant crystalline peaks, but the NMR indicates that there is very little crystalline content. Similarly XRD results show that certain samples are phase mixtures of  $\beta$ -quartz<sub>ss</sub> and  $\beta$ -spodumene<sub>ss</sub> that cannot be resolved by NMR, and consequently it is unwise to interpret the  $^{29}\text{Si}$  MAS NMR spectra of such samples quantitatively. These results emphasise that it is easy to misinterpret one set of data taken in isolation. Both XRD and NMR clearly show that the thermal stability of the  $\beta$ -quartz<sub>ss</sub> is improved by incorporation of nitrogen since this phase persists to higher temperatures in these materials compared to the pure oxide system. Furthermore the effects of using AlN and  $\text{Si}_3\text{N}_4$  as the nitrogen source on the structure and stability of crystalline phases formed are clearly different. It is important to remember that as well as incorporating nitrogen into the system the different nitrogen sources also have the effect of changing the Li:Si:Al ratio. At 1000 °C the samples with AlN give  $^{29}\text{Si}$  MAS NMR spectra of  $\beta$ -quartz<sub>ss</sub> but with increased intensity from  $\text{Q}^4(m\text{Al})$  peaks with higher  $m$  as the aluminum content increases. The  $^{27}\text{Al}$  spectra make an interesting comparison as both XRD and  $^{29}\text{Si}$  NMR clearly confirm the samples to be crystalline, but the  $^{27}\text{Al}$  spectra show a distribution of quadrupolar param-

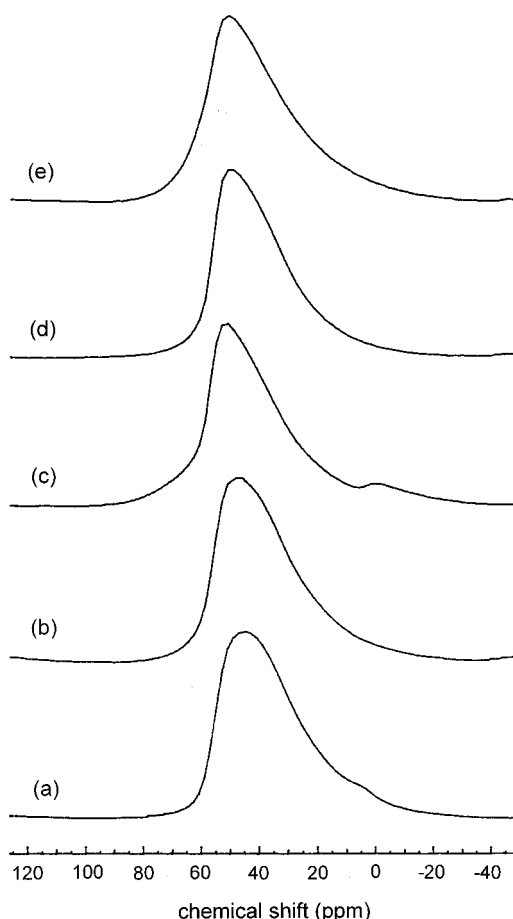


**Figure 4.**  $^{27}\text{Al}$  MAS NMR spectra of (a)  $\beta$ -quartz<sub>ss</sub> and (b) 2NAN, (c) 4NAN, (d) 2NSN, and (e) 4NSN samples heat-treated at 1000 °C.

eters which must arise from atomic disorder and not structural disorder. 4NAN shows evidence of a secondary phase which according to  $^{29}\text{Si}$  NMR must have some nitrogen nearest neighbors (nn). Similarly the  $^{27}\text{Al}$  NMR shows some  $\text{AlO}_6$  content in this sample. It is also clear that although nitrogen is added in the form of AlN, the NMR spectrum shows that no AlN remains as there would be a peak close to 110 ppm. Likewise, the absence of a peak at approximately -50 ppm in the  $^{29}\text{Si}$  NMR spectra, which would be indicative of a local  $[\text{SiN}_4]$  environment, suggests that no residual  $\text{Si}_3\text{N}_4$  is present in any of the samples prepared from  $\text{Si}_3\text{N}_4$ . XRD indicates that sialon X-phase and  $\text{Si}_2\text{N}_2\text{O}$  are present and these have reported  $^{29}\text{Si}$  resonances at -56.5 and -63 ppm, respectively,<sup>29,30</sup> which correspond to  $\text{SiO}_2\text{N}_2$  and  $\text{SiN}_3\text{O}$  local environments. The X-phase has  $^{27}\text{Al}$  NMR signals at 59 and 2.8 ppm which correspond to  $\text{AlO}_4$  and  $\text{AlO}_6$  sites.<sup>19,29</sup> From XRD as well as  $^{29}\text{Si}$  and  $^{27}\text{Al}$  NMR data for samples with  $\text{Si}_3\text{N}_4$  added there is little evidence for any secondary phases except for some corresponding to a peak at -60 ppm in 4NSN at 1200 °C. However, the  $^{29}\text{Si}$  NMR does show that in both 2NSN and 4NSN at 1000 °C there is significant glass content, being completely dominant for 4NSN. The peak position of 4NSN at -95 ppm is the same as that observed in the pure oxide as-cast glass,<sup>28</sup> but in the nitrogen-containing system the resonance extends to

(29) Smith, M. E. *Solid State NMR* **1994**, 3, 111.

(30) Dupree, R.; Lewis, M. H.; Leng-Ward, G.; Williams, D. S. *J. Mater. Sci. Lett.* **1985**, 4, 393.

more positive shift,  $-60$  ppm as compared to  $-80$  ppm, which is a definite indication that nitrogen is becoming incorporated in the glass. For 2NSN heated at  $1000$   $^{\circ}\text{C}$  there is also a characteristic  $\beta$ -quartz<sub>ss</sub> spectrum, and if the broad underlying glass intensity is subtracted off (note undetected by XRD), then peaks with lower  $m$  value are more intense than in a stoichiometric oxide sample. The  $^{27}\text{Al}$  NMR spectra from the NSN samples are again less informative simply showing a main peak from  $\text{AlO}_4$  with the positive edge of the 4NSN sample less well defined, perhaps indicative of increased Al–N bonding.

The implications of these observations are that with increasing  $\text{Si}_3\text{N}_4$  content there is a tendency for the glassy components to resist crystallization. Although the presence of nitrogen has been shown to extend the glass-forming region in other systems by increasing the melt viscosity and inhibiting the nucleation of pure silicate phases, the current results are also consistent with the glass having increased silicon content, a network former compared to aluminum, an intermediate. When AlN is added, the  $^{29}\text{Si}$  MAS NMR spectra obtained from the  $1000$   $^{\circ}\text{C}$  samples are clearly indicative of  $\beta$ -quartz<sub>ss</sub> but with an apparent increase in the relative intensity of  $\text{Q}^4(m\text{Al})$  species with higher  $m$ -values (i.e., silicon sites with more  $nnn$  aluminums). The underlying structure of the  $\beta$ -quartz<sub>ss</sub> appears unchanged from the constancy of the isotropic chemical shifts but with changing Si/Al ratio. The question remains what is the nitrogen solubility in the  $\beta$ -quartz<sub>ss</sub>. From  $^{27}\text{Al}$  NMR there is evidence that some Al–N bonds, such as in  $\text{AlO}_3\text{N}$  groups, exist.<sup>25–27</sup> There is an effect of nitrogen on both the aluminum and silicon resonances producing some weak ill-defined intensity at more positive chemical shift which is *not* present in the pure oxide samples. From all the previous work on oxynitride materials, it is well-known that nitrogen has the effect of decreasing the shielding of these resonances.<sup>24–26,30</sup> Although the silicon:aluminum ratio differs between these samples, the shift of this weak intensity is larger than would be expected to originate from this source alone. Thus it would appear that nitrogen is incorporated in the framework of the majority phase. There is also no doubt that the secondary phases present, X-phase and  $\text{Si}_2\text{N}_2\text{O}$ , have significant nitrogen content, and it is interesting to note that 4NSN and 4NAN samples have very similar amounts of secondary phase.

The most interesting comparison is for the series with varying AlN content. There are three points to note: (i) the tail to positive shift indicating nitrogen content appears only after AlN is added and increases in intensity with nitrogen content, (ii) the increasing amount of secondary phase corresponding to the  $-60$  ppm peak increases with nitrogen content, and (iii) the increasing relative intensity of aluminum-rich  $\text{Q}^n(m\text{Al})$  environments in the  $\beta$ -quartz<sub>ss</sub> structure. Care must be exercised to interpret these intensities even qualitatively. From the main resonance attributed to  $\beta$ -quartz<sub>ss</sub>, even though there may be some overlap with  $nn$  coordination that contain nitrogen, there can be no doubt that silicon environments with more  $nnn$  aluminum in the quartz structure are being formed. This observation needs to be reconciled with the  $\beta$ -quartz<sub>ss</sub> structure and the need to charge-balance. In the case

of the nitrogen-free  $\beta$ -quartz<sub>ss</sub> structure charge-balancing results from the preferential location of  $\text{Li}^+$  ions near tetrahedral units in which the Si atom has been replaced by an Al atom. The substitution of  $\text{Al}^{3+}$  for  $\text{Si}^{4+}$  leads to an excess negative charge that is balanced by the  $\text{Li}^+$  ion so that electrical neutrality is maintained. In the current samples it is believed that this behavior is still in effect since the fundamental  $\beta$ -quartz<sub>ss</sub> structure is retained. However, since the  $^{29}\text{Si}$  NMR spectra of samples prepared from AlN indicate that extra aluminum is entering the  $\text{Q}^4$  framework structure it means that more  $[\text{Al}(\text{O},\text{N})_4]^{x-}$  ( $x \geq 1$ ) units form, and hence excess negative charges are introduced into the system. Since the lithium content is fixed by the initial stoichiometry and is therefore unavailable to compensate for this imbalance, another charge-balancing mechanism must be in operation. One possibility is that some of the lithium sites (which have a one in three occupancy) are occupied by some of the excess  $\text{Al}^{3+}$  ions. Such occupation schemes have been observed in other  $\text{Li}_2\text{O}$ – $\text{Al}_2\text{O}_3$ – $\text{SiO}_2$  compositions. For example in  $\text{Li}_4\text{SiO}_4$  the replacement  $3\text{Li}^+/\text{Al}^{3+}$  is possible giving the solid solution  $\text{Li}_{4-3y}\text{Al}_y\text{SiO}_4$ .<sup>31</sup> A very similar process could be occurring here and is further complicated by the presence of nitrogen in the  $\beta$ -quartz<sub>ss</sub> structure. Another possibility is that some of the excess  $\text{Al}^{3+}$  ions occupy the interstitial sites of the  $\beta$ -quartz<sub>ss</sub> structure so that the  $\text{Al}^{3+}$  ions balance the excess negative charge associated with  $[\text{Al}(\text{O},\text{N})_4]^{x-}$  units. This necessarily requires some of the Al atoms that are introduced from AlN to be in  $[\text{AlO}_6]$  coordination. Such octahedral coordination is in fact observed in the  $^{27}\text{Al}$  NMR spectra (Figure 4) for samples with high AlN content, although the possibility that this  $[\text{AlO}_6]$  peak arises from octahedral sites in the X-phase cannot be discounted.

Thus it would appear given the increasing intensity of higher  $m$  resonances for  $\text{Q}^4(m\text{Al})$  that with increasing AlN content additional aluminum occupies  $\beta$ -quartz<sub>ss</sub> framework sites and that charge-balancing is partially accounted for by aluminum occupying nonframework sites. The complexity of such an altered  $\beta$ -quartz<sub>ss</sub> structure may increase the difficulty for it to convert to  $\beta$ -spodumene<sub>ss</sub>. It is generally thought that  $\text{Si}^{4+}$  does not play the role in the interstitial sites, and hence this may explain why the  $\beta$ -quartz<sub>ss</sub> phase crystallized from  $\text{Si}_3\text{N}_4$ -containing samples is less stable than that in the samples with AlN addition. For 4NAN where  $\beta$ -quartz<sub>ss</sub> remains stable up to  $1300$   $^{\circ}\text{C}$ , there is increasing formation of a separate phase that clearly has significant nitrogen content. The implication is that nitrogen must be separating from the  $\beta$ -quartz<sub>ss</sub> structure prior to its incorporation within the secondary phase, and this may well be a significant factor in determining the high thermal stability of  $\beta$ -quartz<sub>ss</sub> in this sample.

## Conclusion

The effect of  $\text{Si}_3\text{N}_4$  and AlN on the structure of glass–ceramics derived from the  $\text{Li}$ – $\text{Si}$ – $\text{Al}$ – $\text{O}$ – $\text{N}$  system has been studied using XRD and  $^{29}\text{Si}$  and  $^{27}\text{Al}$  MAS NMR. The main crystalline phases formed were  $\beta$ -quartz<sub>ss</sub> and  $\beta$ -spodumene<sub>ss</sub>, although minor amounts of  $\text{Si}_2\text{N}_2\text{O}$  and X-phase were observed in some samples. No NMR peaks corresponding to residual AlN or  $\text{Si}_3\text{N}_4$  were

present, and less glass was observed in samples prepared from AlN compared with samples in which  $\text{Si}_3\text{N}_4$  was used. A 20 ppm extension of the  $^{29}\text{Si}$  resonance, from  $-60$  ppm in 4NSN heat-treated at  $1000$   $^{\circ}\text{C}$  compared to  $-80$  ppm in the pure oxide glass, indicated that nitrogen entered the glass structure. The thermal stability of  $\beta\text{-quartz}_{\text{ss}}$  was improved by incorporating AlN and  $\text{Si}_3\text{N}_4$ , although AlN was more effective than  $\text{Si}_3\text{N}_4$ . This suggests that the retention of  $\beta\text{-quartz}_{\text{ss}}$  to higher temperatures was due not only to the replacement of oxygen by nitrogen but also to the effect of the accompanying cation. In addition, the Si:Al ratio of the majority  $\beta\text{-quartz}_{\text{ss}}$  phase changed as AlN was added, showing an increasing relative intensity of Al-rich  $\text{Q}^n(m\text{Al})$  environments. It is proposed that charge balancing in these materials occurs via the incorporation of a fraction of  $\text{Al}^{3+}$  ions into interstitial sites which, in

conjunction with the replacement of oxygen by nitrogen, complicates the  $\beta\text{-quartz}_{\text{ss}}$  structure and restricts its tendency to transform to  $\beta\text{-spodumene}_{\text{ss}}$ .

**Acknowledgment.** The authors thank Gwalia Australia Ltd. for supplying the raw mineral used in this study and Dr. Tim Bastow (CSIRO Division of Materials Science and Technology) for providing access to the Bruker MSL 400 spectrometer. Thanks are also extended to Dr. Maria Forsyth (Monash University) for performing some of the NMR experiments and to the Monash Research Fund Grant for enabling the purchase of the Bruker CXP 300 spectrometer used in this work. A.N. is grateful to the Australian Government and Monash University for financial support.

CM960238F